Chapter 2

Synthesis of Alkene 23

2 Synthesis of Alkene 23

2.1 Synthesis of AA Substrate

Alkene **28** was constructed from *p*-anisic acid **38** (Figure 2.1) using similar conditions to Hung Duong (Chapter 1, page **Error! Bookmark not defined.**). The esterification worked well using a modified procedure[28] to form allyl ester **39** with improved yield. Purification of the product was easily achieved by eluting the crude product through a short plug of silica.

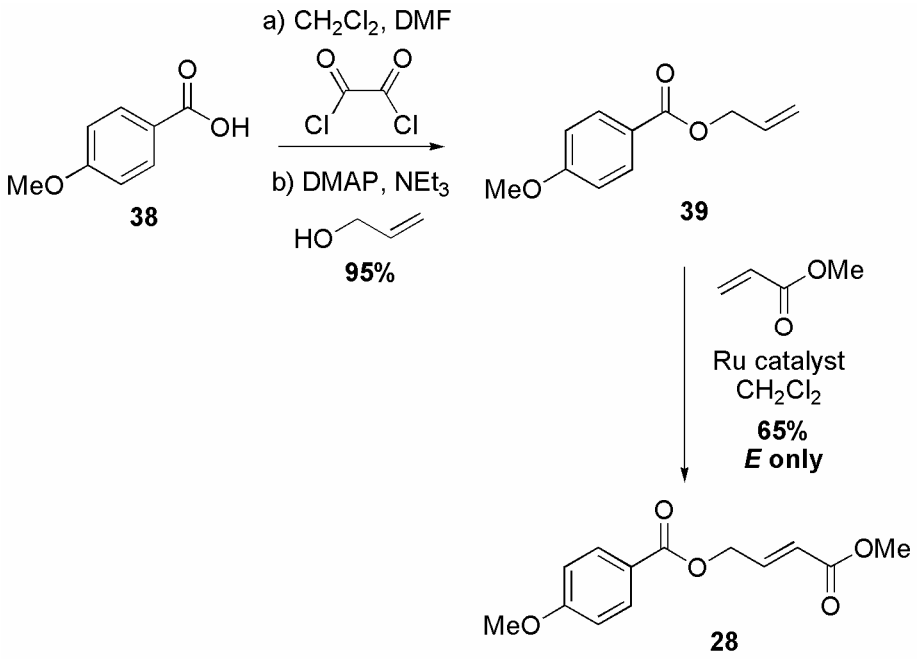

Figure 2.1 Initial synthesis of alkene **28**.

Cross metathesis of allyl ester **39** with methyl acrylate using Grubb's second generation catalyst (Figure 2.2) was highly selective for the desired (*E*)-alkene ***E*-28** but proved troublesome on larger scales. Purification problems were encountered resulting in residual catalyst contamination. Moderate, irreproducible yields were obtained that were not enhanced by heating the reaction at reflux in toluene.[29] Cross metathesis is a very effective method of producing (*E*)-alkenes on small scales however on the large scale required for this project the cost ($839 AUD / 2 g as on 06/09/2005)[20] of the ruthenium catalyst linked with purification

problems rendered the reaction unsuitable for the synthesis. Alternative routes using Wittig olefination and Horner-Wadsworth-Emmons (HWE) olefination were investigated.

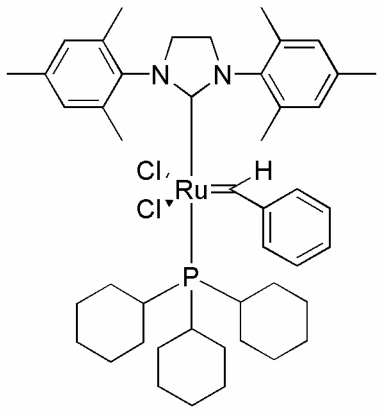

Figure 2.2 Grubb's second generation catalyst.

The Wittig olefination (Figure 2.3) couples a phosphorus ylide **42** with a carbonyl compound **43** eliminating a phosphine oxide to afford a mixture of (*E*)- and (*Z*)-alkenes **44**.

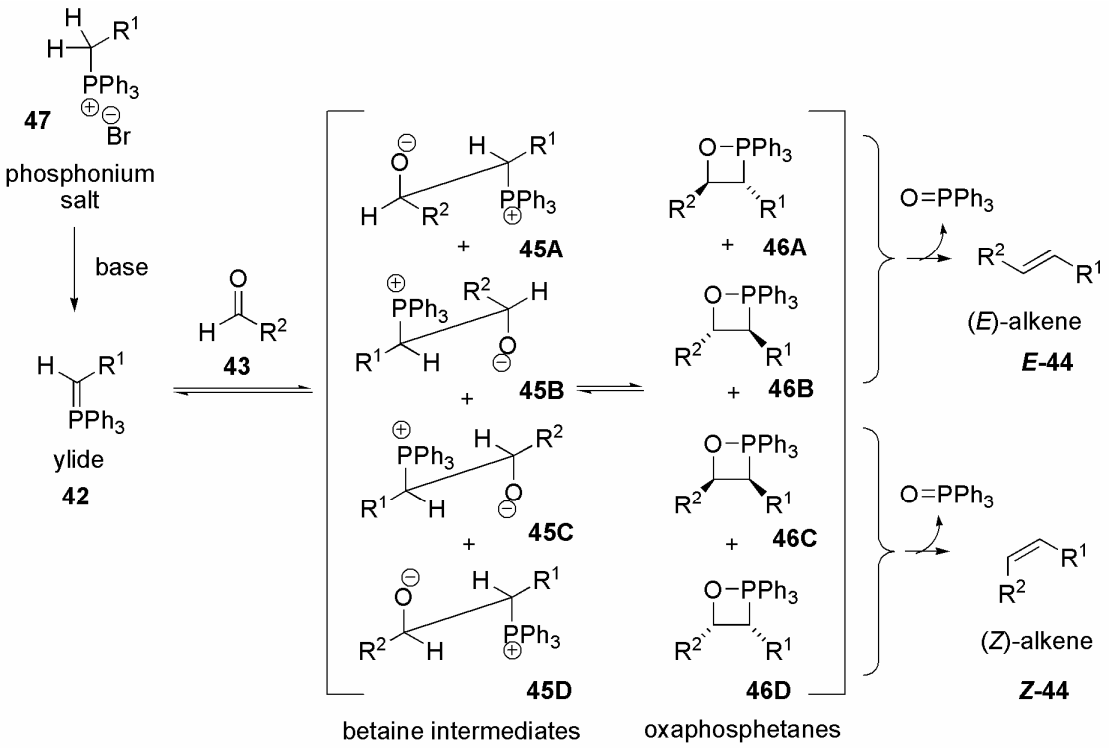

Figure 2.3 Mechanism of the Wittig reaction.

The mechanism is thought to involve addition of ylide **42** to carbonyl compound **43** to form a betaine intermediate. There are four possible ways that these two compounds could add forming betaine intermediates **45A**, **45B**, **45C** and **45D**. Each betaine intermediate cyclises specifically to its corresponding oxaphosphetane **46A**, **46B**, **46C** and **46D**. The *trans*-oxaphosphetanes **46A** and **46B** eliminate triphenylphosphine oxide to afford (*E*)-alkene ***E*-44** while *cis*-oxaphosphetanes **46C** and **46D** eliminate triphenylphosphine oxide to afford (*Z*)-alkene ***Z*-44**. When a stabilised phosphorus ylide (eg. $R^1 = CO_2Me$) is required it can be preformed by reaction of the phosphonium salt **47** with sodium hydroxide, then isolated and added to the reaction as the ylide **42**. When an unstabilised phosphorus ylide (eg. $R^1 = CH_2R$) is required it is formed *in situ* by treatment of the phosphonium salt **47** with a strong base before addition of the aldehyde **43**.

It was envisaged that alkene **28** could be formed by coupling phosphorus ylide **48** with aldehyde **49** in a Wittig reaction. Stabilised phosphorus ylide **48**[68] was prepared by reaction of triphenylphosphine with methyl bromoacetate and subsequent deprotonation of the resulting phosphonium salt using dilute aqueous sodium hydroxide solution (Figure 2.4).

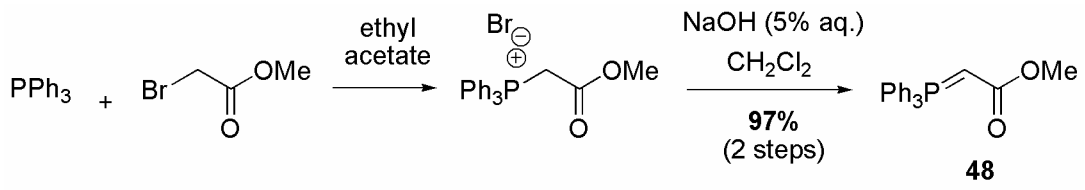

Figure 2.4 Preparation of stabilised ylide **48**.

Aldehyde **49**[61] was formed by oxidation of allyl ester **39** using a catalytic amount of osmium tetroxide and subsequent cleavage of the generated diol using sodium periodate (Figure 2.5). For characterisation purposes, the aldehyde was purified by flash chromatography. This was found to accelerate decomposition and crude aldehyde was used in subsequent reactions with no detrimental effect.

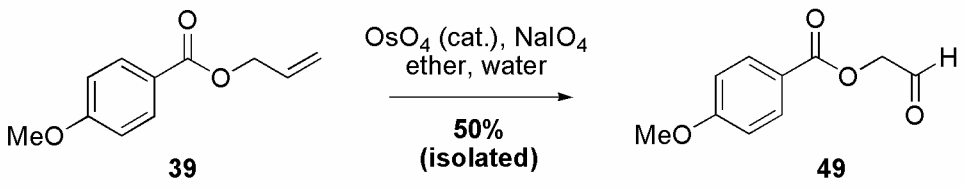

Figure 2.5 Preparation of aldehyde **49**.

Wittig olefination (Figure 2.6) between stabilised ylide **48** and purified aldehyde **49** proceeded in good yield but with poor (*E*)-selectivity (*E* : *Z* = 2 : 1). Alternative HWE chemistry was investigated.

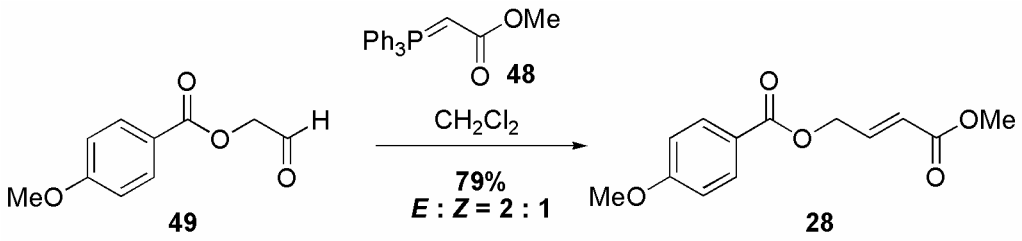

Figure 2.6 Wittig olefination.

The HWE olefination is a variant of the Wittig olefination using a phosphorus anion derived from a phosphonate **50** (Figure 2.7). The anion reacts with an aldehyde **43** to form an alkene **51** *via* a similar mechanism to the Wittig olefination (for the mechanism of the Wittig olefination see Figure 2.3). The anion formed in the reaction is generally more reactive than that of the Wittig reaction and less functional groups are tolerated in the reaction. The benefit of this method is that it is generally very (*E*)-selective.

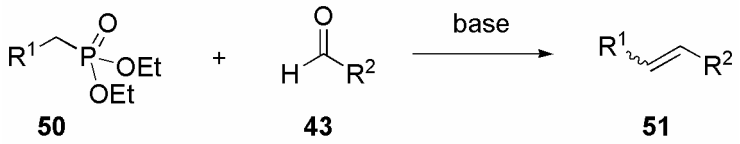

Figure 2.7 Generic HWE olefination.

A HWE reaction between commercially available methyl diethylphosphonoacetate **52** (Figure 2.8) and crude aldehyde **49** formed alkene **28** in excellent yield with good (*E*)-selectivity (*E* : *Z* = 25 : 1). The isomers were easily separated by flash chromatography and pure (*E*)-alkene ***E*-28** was obtained in synthetically useful levels for further elaboration.

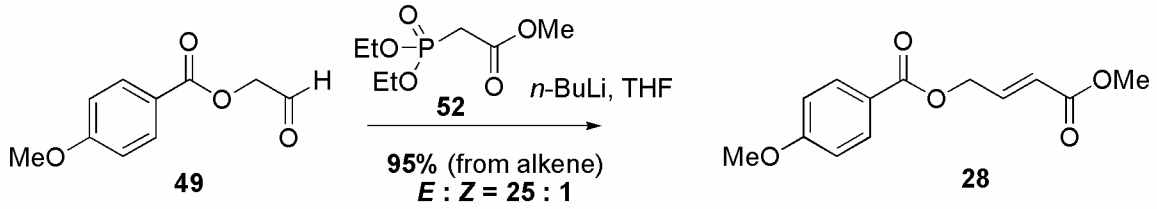

Figure 2.8 HWE reaction.

2.2 The AA

2.2.1 Introduction to the Reaction

The Sharpless Asymmetric Aminohydroxylation (AA) (Figure 2.9) converts an alkene to a protected vicinal aminoalcohol with high regio- and enantio-selectivity.[30] The reaction mechanism (see Figure 2.13) dictates that addition must occur in a *syn* fashion, that is, where both groups add to the same face of the alkene, giving rise to four possible products. If the aminoalcohol adds to the back-face of *trans*-alkene ***E*-51** with the amine group beta to R^2, aminoalcohol **53** is formed. If the amine group ends up alpha to R^2, the regio-isomeric aminoalcohol **54** is formed. Similarly if the aminoalcohol adds to the front-face, enantiomers ***ent*-53** and ***ent*-54** are formed. For this reaction to be synthetically useful both the regio- and enantio-selectivity must be controlled to favour the desired product selectively.

Various protected aminoalcohols – acetamides, carbamates or sulfonamides – can be formed by using a nitrogen source that differs in the *N*-substituent (R^3). The carbamate based AA was chosen because it has been found to react with higher enantio- and regio-selectivity than the alternative methods[30] and the resulting carbamate protecting group can be cleaved under relatively mild conditions.[31]

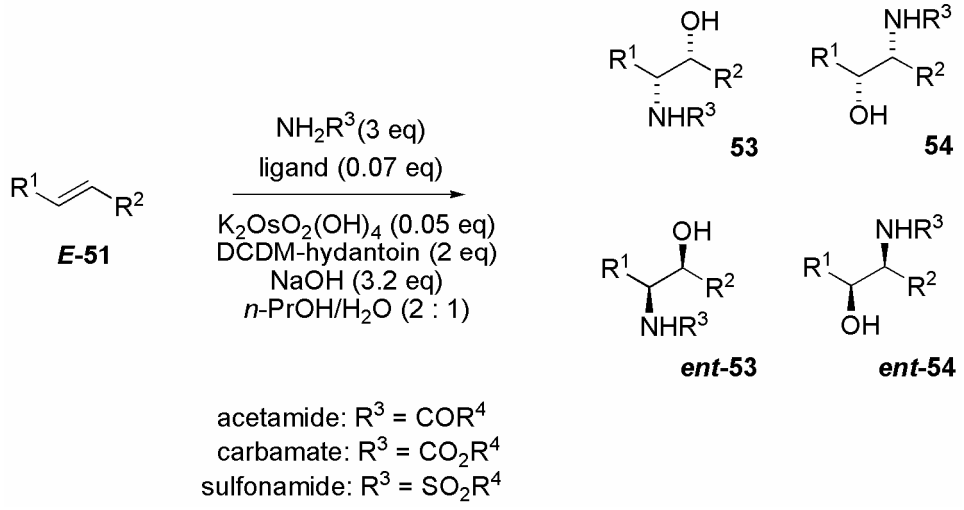

Figure 2.9 Generic AA.

The enantio- and regio-selectivity is ultimately induced in the product when the addition involves the chiral catalyst. The catalyst is generated *in situ* and consists of a reactive imidotrioxoosmium(VIII) species **55** (Figure 2.10) in combination with a chiral *Cinchona* alkaloid derived ligand (Figure 2.11).[30] Imidotrioxoosmium(VIII) species **55** is formed by reaction of carbamate **56** with sodium hydroxide and 1,3-dichloro-5,5-dimethylhydantoin to form chloramine salt **57** which subsequently reacts with potassium osmate.[30] The ligands are made up of an aromatic spacer group, for example phthalazine (PHAL) or anthraquinone (AQN), and a chiral *Cinchona* alkaloid moiety: either dihydroquinine (DHQ) or its pseudo-enantiomer dihydroquinidine (DHQD).[30] In many cases the aromatic linker can strongly influence the regio-selectivity of the reaction, with phthalazine ligands favouring one regio-isomer (**53** and ***ent*-53**) and anthraquinone ligands favouring the other regio-isomer (**54** and ***ent*-54**). The chiral alkaloid induces enantio-selectivity in the reaction by favouring addition to one enantio-topic face of the pro-chiral alkene substrate. The asymmetric induction closely parallels that of the Sharpless Asymmetric Dihydroxylation[32] (AD) and can be predicted using the AD mnemonic.[32] The AD reaction is further explained in Chapter 3. A high degree of regio- and enantio-control can be obtained if substrate-catalyst interaction is maximised through appropriate substrate design and reagent selection.

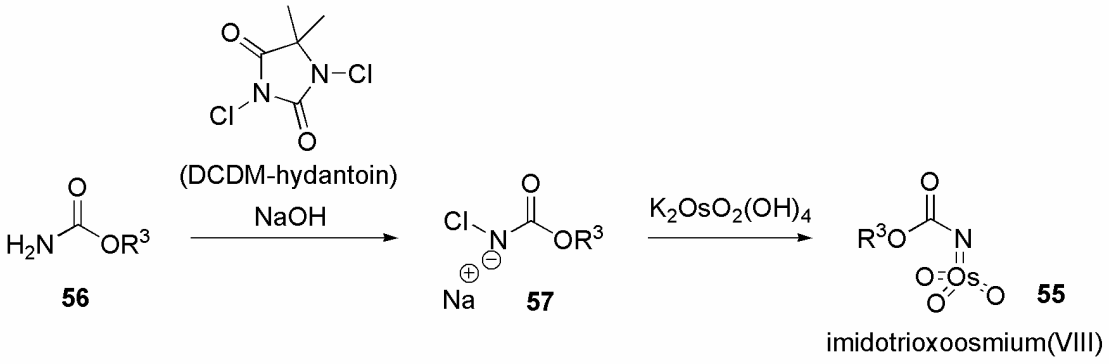

Figure 2.10 Formation of the active osmium species.

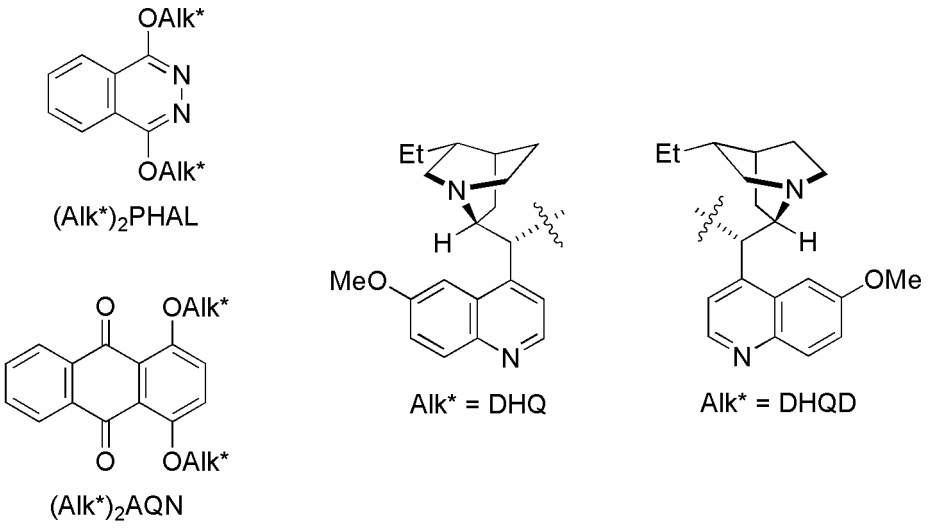

Figure 2.11 Chiral *Cinchona* alkaloid derived ligands.

The AD mnemonic (Figure 2.12) contains steric barriers in the northwest and southeast quadrants whereas the northeast and southwest quadrants are relatively open. To predict the outcome, the alkene must be positioned according to the constraints of the mnemonic; with the small hydrogen substituents of the alkene pointing towards the sterically congested southeast and northwest quadrants.[32] There are two possible substrate orientations A and B and either orientation positions the alkene so that attack from the top or β-face (favoured by DHQD-derived ligands) would lead to products **53** and **54** (for structures see Figure 2.9) while attack from the bottom or α-face (favoured by DHQ-derived ligands) would lead to products ***ent*-53** and ***ent*-54**.

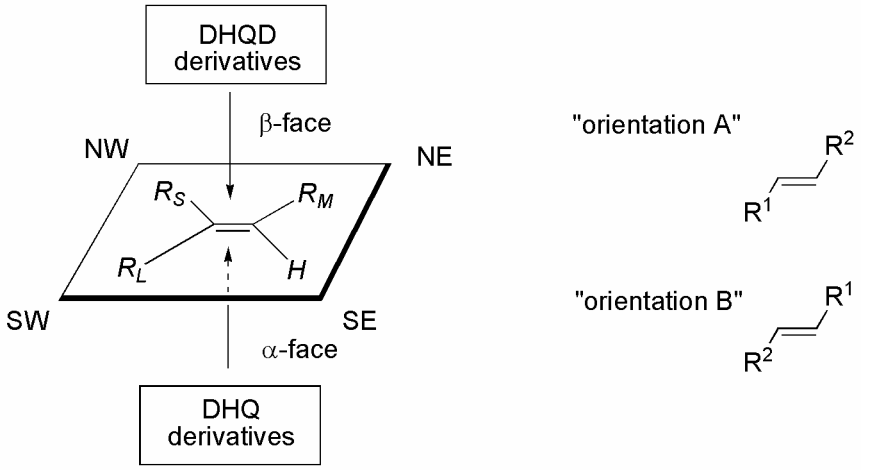

Figure 2.12 AD-mnemonic and substrate orientation.

The AD can occur under the AA reaction conditions and as a result the AA products can often be contaminated with diol products, reducing yield and complicating purification. Diol formation can be reduced by using a high ligand to osmium ratio.

A mechanistic scheme (Figure 2.13) has been proposed for the AA with two competing catalytic cycles[30] where the primary cycle involves the ligand and hence leads to high selectivity while the secondary cycle does not, resulting in addition products with low selectivity. As illustrated in Figure 2.13, ligand-mediated addition of imidotrioxoosmium(VIII) species **55** with *syn*-specificity to the alkene is thought to give azaglycolate **58**. The nitrogen source is thought to re-oxidise azaglycolate **58** to form oxidised-azaglycolate **59** which upon hydrolysis liberates the product and regenerates imidotrioxoosmium(VIII) species **55**, completing the primary cycle. Alternatively, oxidised azaglycolate **59** may enter the secondary cycle by addition to another alkene forming bis(azaglycolate)osmium species **60**. This addition is thought to be independent of the chiral ligand and as a result does not induce regio- or enantio-selectivity in the product and upon hydrolysis, the product is liberated with low selectivity and azaglycolate **58** is regenerated.[30]

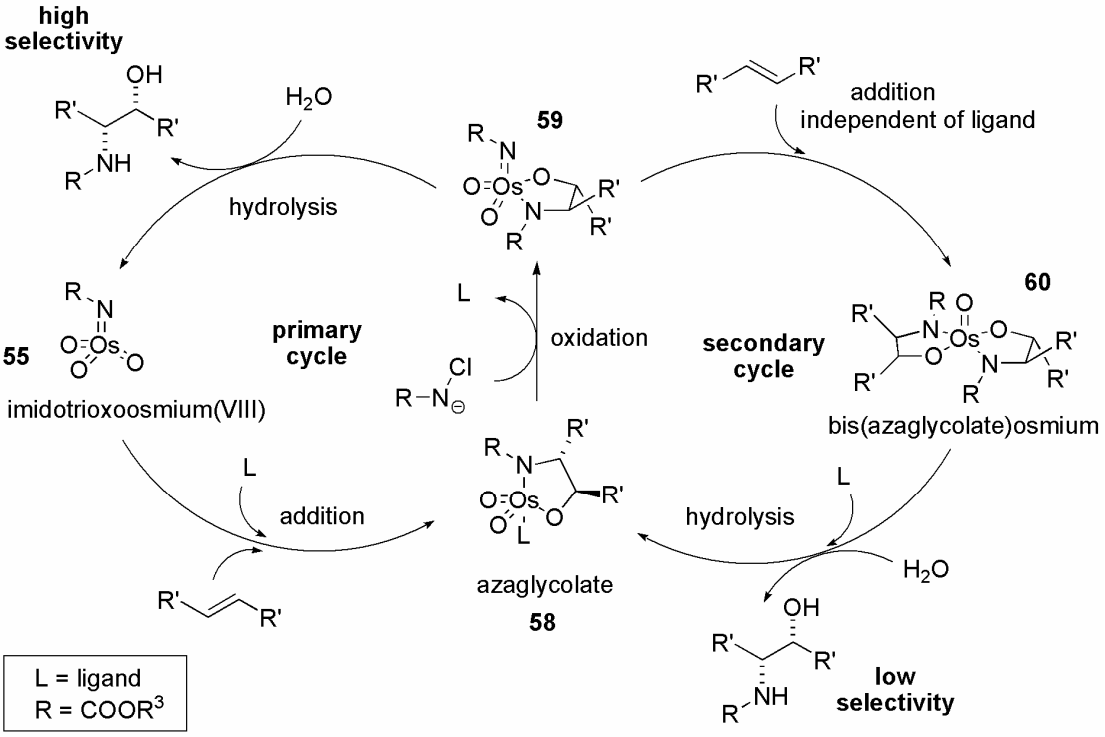

Figure 2.13 Catalytic cycle of the AA.[30]

The ligand has been observed to increase the catalytic turnover of the reaction favouring the primary cycle. The hydrolysis steps limit turnover and have been found to be accelerated by use of aqueous solvent mixtures allowing the primary cycle to dominate. With most systems a 1 : 1 propanol : water mixture has been found to be ideal for maximising hydrolysis while minimising AD diol formation however a 2 : 1 ratio has been found to work best when *tert*-butyl carbamate is used as the nitrogen source.[30]

2.2.2 The Reaction

Commercially available *tert*-butyl carbamate was chosen in preference to other carbamates as the nitrogen source because of its success in previous reactions. It has been found to react with higher enantio- and regio-selectivity than benzyl carbamate and its subsequent cleavage is relatively facile compared to ethyl carbamate.[30] A method[33] for cleavage of methyl carbamates has made it a viable alternative nitrogen source and its use was investigated and reported later in this thesis (Chapter 4, page **Error! Bookmark not defined.**).

The desired product of the AA is β-aminoalcohol **27** (Figure 2.14) where the amine adds beta to the methyl ester and addition occurs to the back face of alkene ***E*-28**. Ideally the formation of enantiomer ***ent*-27**, regio-isomer **61** and its enantiomer ***ent*-61** must be minimised by maximising substrate-catalyst interaction. A number of factors are thought to influence the substrate-catalyst interaction including steric and electronic effects. Previous studies[34] have shown that α,β-unsaturated esters with a small ester group, minimising steric interactions and an aryloxy- group positioned at C_5, optimising favourable pi-stacking interactions with the ligand, afford products with high regio- and enantio-selectivity. The α,β-unsaturated alkene substrate ***E*-28** was designed to include a small methyl ester group and an aromatic *p*-methoxybenzoyl protecting group at C_4. Corey and Noe[35] found that this aromatic group was positioned at the required distance from the alkene for maximum interaction with the catalyst for the AD leading to products with high enantio-selectivity.

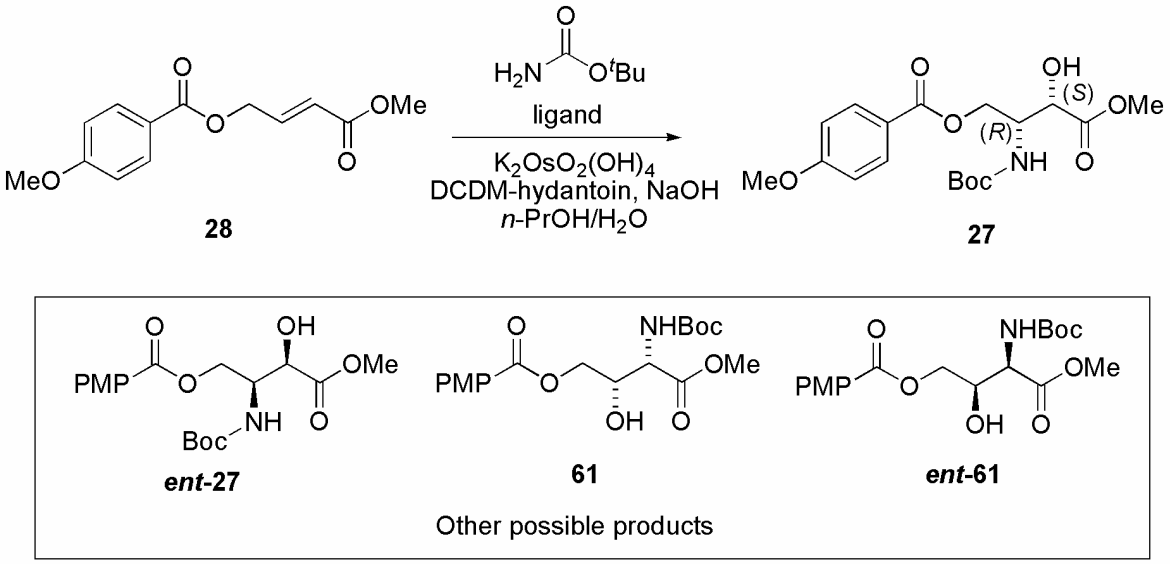

Figure 2.14 The AA.

The chiral ligand $(DHQD)_2PHAL$ was predicted to favour the formation of desired product **27** with chiral alkaloid DHQD favouring the correct enantiomer, as predicted by the AD-mnemonic, and aromatic spacer PHAL favouring the correct regio-isomer, as predicted by comparison with similar systems in the literature.[30] The influence of ligand choice on the reaction was studied (Figure 2.15).

Entry	Ligand	Yield (%)	Regio-selectivity α : β	Major enantiomer	% ee
1	$(DHQD)_2PHAL$	74	β-only	**27**	97*
2	$(DHQ)_2PHAL$	70	β-only	***ent*-27**	98*
3	$(DHQD)_2AQN$	§	1.5 : 1.0#	§	§
4	$(DHQ)_2AQN$	§	1.2 : 1.0#	§	§
5	$(DHQD)_2PYR$	§	1.0 : 1.7#	§	§

*** =** determined by Hung Duong by chiral HPLC of the acetyl derivatives (see Chapter 1, page **Error! Bookmark not defined.**); **§** = not determined; **#** = determined by integration of the N-H peaks in the 200 MHz ^1H NMR spectra of the crude product

Figure 2.15 Ligand effects.

As predicted, the PHAL ligands (entry 1, 2) favoured formation of the β-aminoalcohols in good yield with no α-aminoalcohol product observed. The

enantio-selectivity was high with formation of the desired product **27** strongly favoured by DHQD (97% ee) and formation of the enantiomer ***ent*-27** strongly favoured by DHQ (98% ee). The AQN ligands (entry 3, 4) favoured formation of the regio-isomeric α-aminoalcohols with lower selectivity forming mixtures of α- and β-aminoalcohols. Another ligand with a pyrimidine (PYR) aromatic spacer (entry 5) favoured formation of the β-aminoalcohols but with low selectivity. The enantio-selectivity of the products formed using the AQN or PYR ligands was not determined because the reactions would not be synthetically useful due to low regio-selectivity.

The regio-isomers were readily identified by ^{1}H NMR analysis of the crude product. It has been established that α-aminoalcohol and β-aminoalcohol AA products of α,β-unsaturated substrates show characteristic chemical shifts for the N-H proton: α-aminoalcohols within δ 5.7 – 5.2 ppm and β-aminoalcohols within δ 4.9 – 4.4 ppm (Figure 2.16).[36] In the case of AA products **61** and **27**, a broad doublet at 5.45 ppm in the 200 MHz ^{1}H NMR spectra was assigned to α-aminoalcohol **61** and a broad doublet at 5.03 ppm was assigned to β-aminoalcohol **27**. The regio-selectivity of the reaction was determined by the relative integration of these peaks.

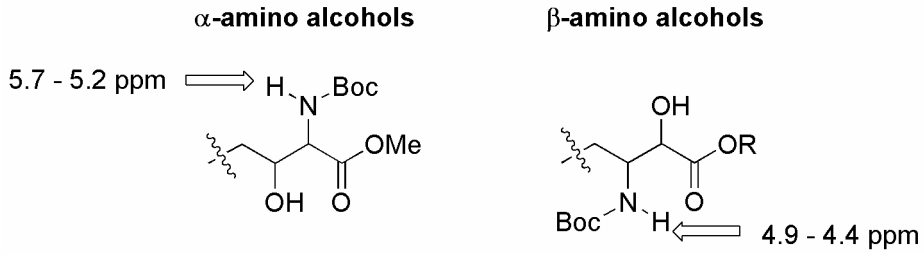

Figure 2.16 Typical ^{1}H NMR chemical shifts of α,β-unsaturated AA substrates.[36]

Further evidence supporting this assignment was obtained by the following Mosher's derivative formation and from the acetyl derivative formed by Hung Duong. The ^{1}H NMR spectra of the AA product **27** and its acetyl derivative **41** (see Chapter 1, page **Error! Bookmark not defined.**) were compared and the signal due to C_2-H in the acetyl derivative **41** was shifted downfield 0.84 ppm and was simplified to a doublet which is consistent with the alcohol group positioned at C_2 but not at C_3 in AA product **27**.

The absolute stereochemical configuration of β-aminoalcohol **27** was predicted to be (2*S*, 3*R*) using the AD mnemonic (see Figure 2.12). The absolute configuration at the C_2 secondary hydroxy was confirmed as (*S*) using "Mosher's" method which was originally proposed by Mosher and Dale[37] and re-established as an effective method by Kakisawa and co-workers.[38] The procedure involves the preparation of both the (*R*)-α-methoxy-α-trifluoromethylphenylacetate (MTPA) and (*S*)-MTPA esters of the secondary hydroxy to form diastereomeric compounds ***R*-62** and ***S*-62** (Figure 2.17). It has been proposed that these esters adopt a specific conformation in solution where the carbinyl hydrogen (C_2-H), trifluoromethyl group and ester carbonyl of the MTPA moiety line up in the same plane (the plane of the page in Figure 2.17). The phenyl of the MTPA ester shields protons that are on the same side of the plane as it. If C_2 had the predicted (*S*)-configuration the signals due to the CO_2Me group would be shielded in (*R*)-Mosher ester ***R*-62** relative to that in (*S*)-Mosher ester ***S*-62** giving a negative chemical shift difference (Δδ where Δδ = δ_R-δ_S in ppm). The protons attached to C_3 and C_4 and the substituents that branch from these carbons would be shielded in ester ***S*-62** relative to that in ester ***R*-62** giving a positive Δδ. If C_2 had an (*R*)-configuration the opposite shielding would be observed.

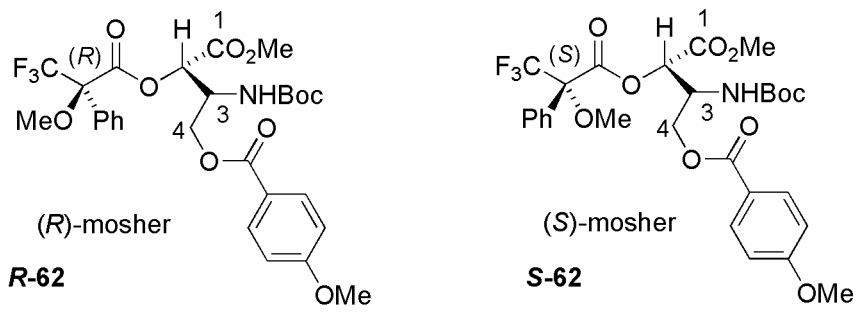

Figure 2.17 Mosher's esters of AA product.

In each reaction the formation of only one product was detected in the ^{1}H NMR spectra of the crude product. This observation supports the high enantio-selectivity (> 95% ee) assigned by chiral HPLC. The ^{1}H NMR spectra of the purified esters were assigned using COSY correlations and the chemical shifts differences were calculated (Figure 2.18). The arrangement of positive and negative Δδ's confirmed C_2 was the (*S*)-configuration. The configuration at C_3 was

assigned as (*R*)- because the AA is known to install an aminoalcohol *via* a concerted *syn* addition with complete stereo-specificity.

Proton	δ_R (*R*)-MTPA ester ***R*-62**	δ_S (*S*)-MTPA ester ***S*-62**	$\Delta\delta$ (δ_R-δ_S)
CO_2CH_3	3.77	3.80	-0.03
C_3-H	4.82 – 4.74	4.77 – 4.64	+0.07*
N-H	4.82 – 4.74	4.77 – 4.64	+0.07*
BOC $C(CH_3)_3$	1.40	1.39	+0.01
C_4-H_A	4.43 – 4.35	4.30 – 4.17	+0.16*
C_4-H_B	4.21 – 4.10	3.88 – 3.84	+0.30*
o-Ar-H	8.00 – 7.93	7.98 – 7.91	+0.02*
m-Ar-H	6.96 – 6.89	6.96 – 6.89	0.00
Ar-OCH_3	3.86	3.86	0.00

* = $\Delta\delta$ was calculated from the midpoints of the multiplets

Figure 2.18 Relative shifts in the 200 MHz ^{1}H NMR spectra of Mosher's esters **62**.

In summary, the desired β-aminoalcohol **27** was formed using $(DHQD)_2PHAL$ in good yield with very high regio- and enantio-selectivity. An investigation into protecting group strategies for the newly created aminoalcohol was undertaken.

2.3 Elaboration to Olefination Precursor

Aminoalcohol **27** was protected as TBDMS-ether **63** (Figure 2.19) via two different procedures. Long reaction times, up to seven days, were required to give good conversion when TBDMS-chloride was used as the source of the protecting group. Similar conversion was obtained within one day when the more reactive TBDMS-triflate was used.

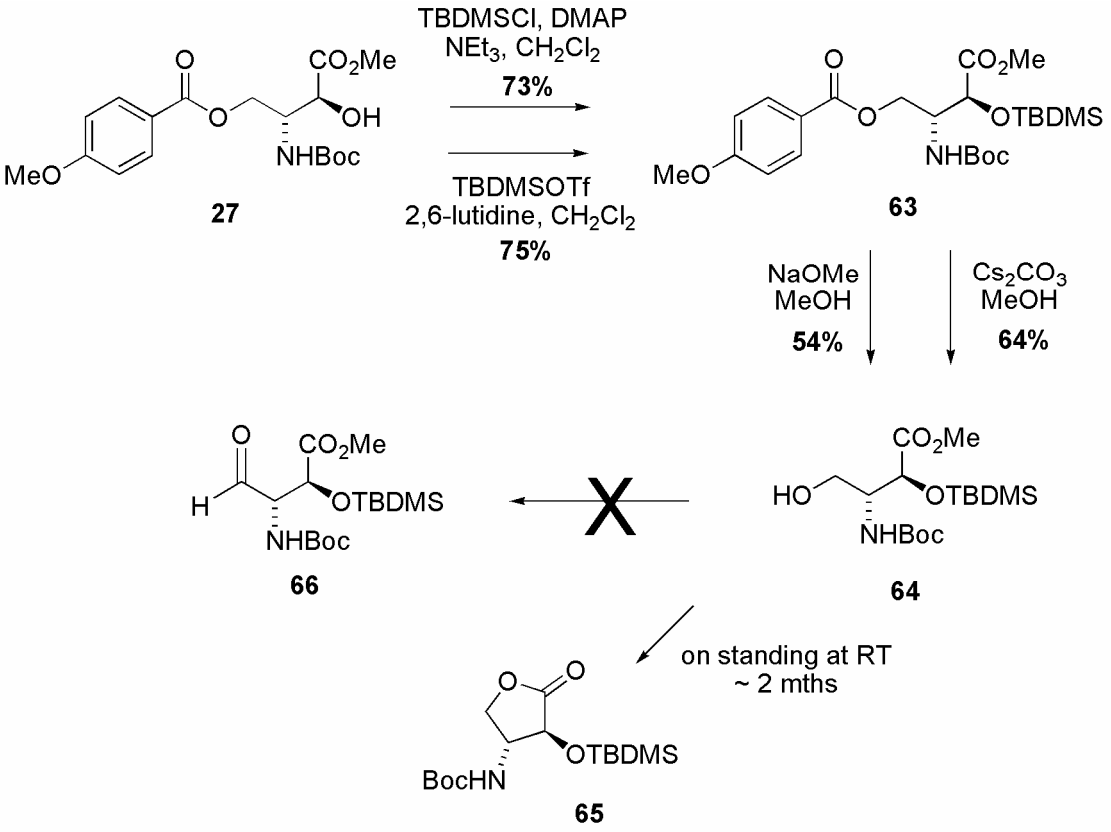

Figure 2.19 TBS protection route.

The *p*-methoxybenzoyl protecting group was subsequently removed by trans-esterification of ester **63** using methoxide, formed from either sodium methoxide or caesium carbonate in methanol. The reaction was hard to monitor by TLC because the methyl 4-methoxybenzoate by-product co-eluted with the starting material. The caesium carbonate method was favoured because of the ease of reagent manipulation and alcohol **64** was formed in moderate yield. It was noted that a sample of alcohol **64** that was left standing at room temperature for some time completely and cleanly converted to lactone **65**.

Attempts to convert alcohol **64** into aldehyde **66** were not successful. Standard Dess-Martin, Swern with either aqueous workup[39] or anhydrous workup[40], and SO_3-pyridine oxidation[41] procedures failed to form any aldehyde after workup. ^{1}H NMR analysis of the crude products indicated the absence of aldehyde **66**, alcohol **64** or lactone **65** and the presence of unassigned decomposition products. It was postulated that the presence of the N-H was causing problems and an alternative protecting strategy was investigated.

An oxazolidine protecting group was chosen to form 2,2-dimethyloxazolidine **67** under acid-catalysed conditions (Figure 2.20). This protecting group was chosen because it is relatively small which would hopefully allow effective substrate-catalyst interaction in the subsequent AD, and it simultaneously protects the hydroxy and the amine. The ring formed holds the methyl ester and the C_4-hydroxy group far apart in a *trans*-related conformation to prevent formation of products like lactone **65** (see Figure 2.19) later in the synthesis.

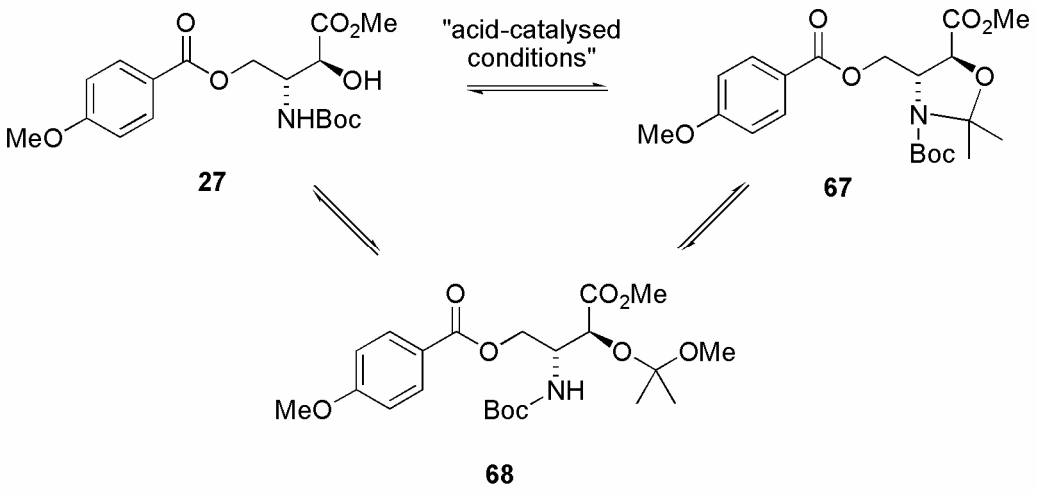

Figure 2.20 N,O-acetal protection.

An initial attempt to form oxazolidine **67** using 2,2-dimethoxypropane (2,2-DMP) worked with poor conversion and a significant amount of alcohol **27** and a small amount of intermediate **68** were recovered (Figure 2.21, entry 1). The products were easily separable by gradient flash chromatography and recovered alcohol **27** was re-exposed to the reaction. An alternative source of the protecting group, 2-methoxypropene (2-MP), provided better conversion with reduced reaction time and temperature (entry 2). The formation of non-polar contaminants was observed using this reagent but these were easily removed using gradient flash chromatography.

The presence of an equilibrium reaction was detected when isolated oxazolidine **67** was exposed to the reaction conditions and was converted to a mixture of alcohol **27** and oxazolidine **67** in a 1 : 2.5 ratio. When pure intermediate **68** was exposed to the reaction conditions, a similar ratio of products was obtained. It was proposed that removal of by-product methanol from the reaction should drive the equilibrium towards the desired product. Attempts to remove methanol from the

reaction by addition of 5 Å molecular sieves directly to the reaction mixture or by use of a Dean-Stark apparatus containing 5 Å molecular sieves suspended in the solvent, failed to increase the conversion to product. Various other activating acids (boron trifluoride diethyl etherate or 10-camphorsulfonic acid), solvents (dichloromethane), temperatures (0 °C to 150 °C) and times (2 h to 7 days) failed to improve the conversion.

Entry	Reagent	Acid	Solvent	Temp. (°C), (Time (h))	Yield of Products (%)			
					27	**68**	**67**	**69**
1	2,2-DMP	TsOH	benzene	95 (32)	43	1.6	39	-
2	2-MP	TsOH	benzene	0 (2), RT (5)	22	-	60	-
3	2-MP	PPTS	toluene	RT (1)	-	98	-	-
4	2-MP	PPTS	toluene	RT (1), 110 (3)	-	-	76	20
5	2-MP	PPTS	toluene	RT (20), 125 (18)	15	-	52	30
6	2-MP	PPTS	toluene	150 (1), 135 (24)	13	-	11	75
7*	2-MP	PPTS	toluene	RT (2)[§], 110 (3)	14	-	85	-

***** = the reaction was attempted once. In subsequent overall yield calculations, the yield from entry 4 was used; **§** = the excess of 2-MP was removed under reduced pressure prior to heating the reaction above room temperature

Figure 2.21 Conditions for oxazolidine formation.

An alternative activating acid, pyridinium *p*-toluenesulfonate (PPTS)[42] was used and essentially complete conversion to intermediate **68** was observed after 1 h at room temperature (entry 3). The reaction was then heated at 110 °C for 3 h and product **67** was formed in a synthetically useful yield (entry 4). No alcohol **27** or intermediate **68** were recovered however the formation of a new compound with similar polarity and spectral data to the product was observed. Initially it was thought that epimerisation had occurred however extensive NMR analysis identified the compound as by-product **69** (see Figure 2.22).

It was postulated that by-product **69** may form via two pathways (Figure 2.22). Path A involves reaction of alcohol **27** with a 2-methoxypropene dimer **70** that is likely to form under the acidic reaction conditions, to generate intermediate **71** that

cyclises to by-product **69**. Path B involves reaction of intermediate **68** with a second 2-methoxypropene molecule to form intermediate **72** that cyclises to by-product **69**. While neither intermediate **71** nor intermediate **72** were isolated from the reaction, in reactions where full conversion to the intermediate is carried out prior to heating it is likely that the reaction proceeds *via* Path B. It was interesting to note that only one of the two possible diastereo-isomers of by-product **69** was formed but the exact stereochemistry was not determined.

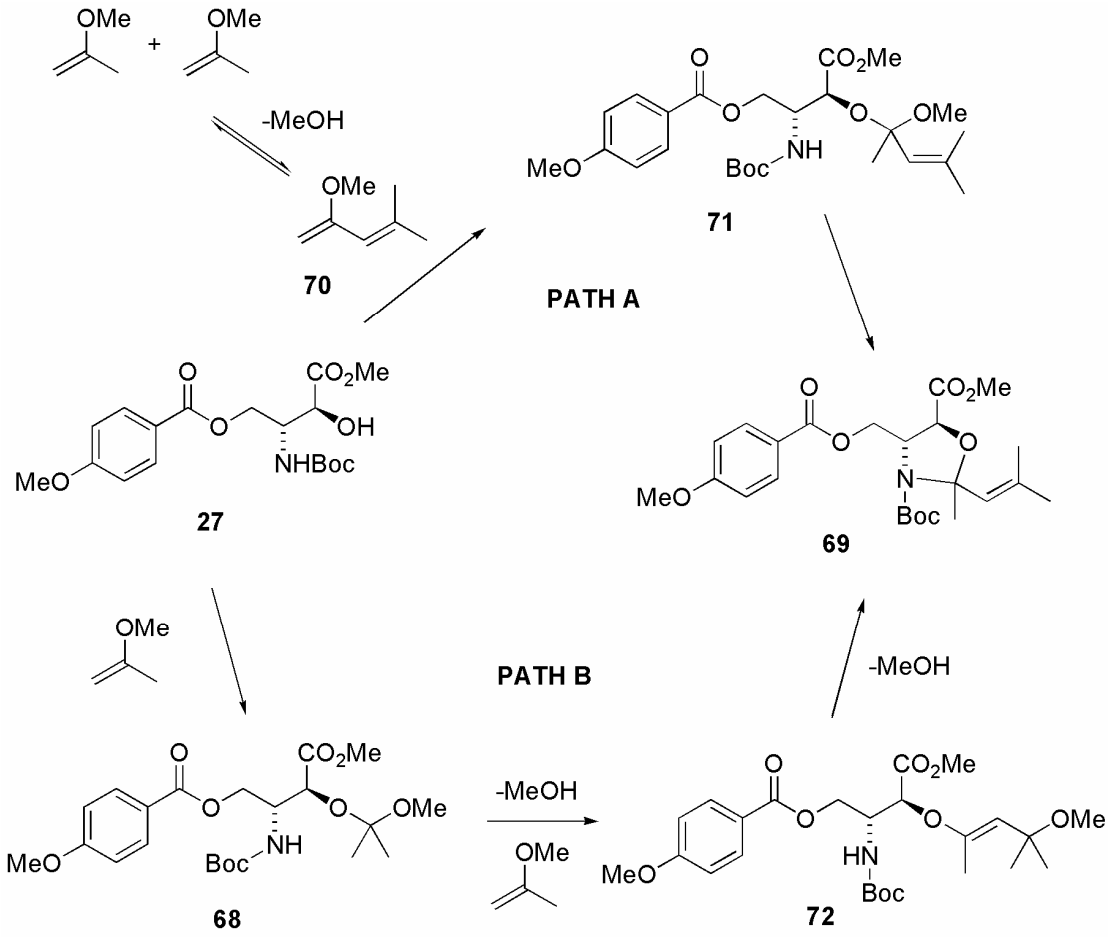

Figure 2.22 Proposed formation of by-product **69**.

By-product **69** was readily de-protected back to alcohol **27** using PPTS in methanol (Figure 2.23) and this material was recycled back into the synthesis.

In an attempt to reduce formation of by-product **69**, the reaction was repeated with a lower reaction temperature of 70 °C however significant amounts of alcohol **27** and intermediate **68** were recovered. Longer reaction time (Figure 2.21, entry 5) and increased temperature (entry 6) were found to increase formation of by-product **69**. It was proposed that if the excess of 2-MP was removed from the

reaction prior to heating, formation of by-product **69** could be avoided. Indeed when the low-boiling point volatiles (2-MP: **lit.**[43] **b.p.** 34 – 36 °C) were removed under reduced pressure before heating the reaction, no by-product **69** was observed and an improved yield was obtained (entry 7). The reaction may be further improved by using 2,2-DMP in conjunction with PPTS.

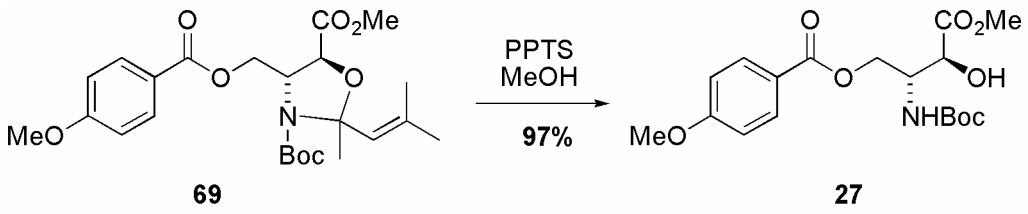

Figure 2.23 By-product deprotection.

The *p*-methoxybenzoyl protecting group of pure oxazolidine **67** was removed by trans-esterification using caesium carbonate in methanol to give alcohol **73** in good yield (Figure 2.24). By-product **69** sometimes contaminated the starting material due to incomplete separation in the previous step and as a result by-product alcohol **74** (see Figure 2.25) was found to contaminate the product. The alcohols were easily separated by flash chromatography and pure alcohol **73** was reacted further. The identity of by-product alcohol **74** was confirmed by de-protection of pure by-product **69** to form pure by-product alcohol **74** (Figure 2.25). Alcohol **74** was found to be relatively unstable and immediate separation was found to be advantageous.

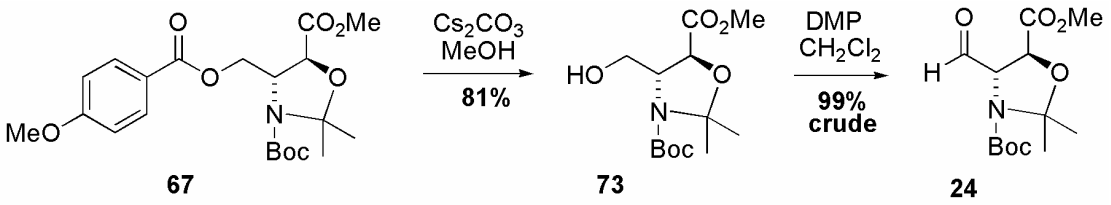

Figure 2.24 Trans-esterification of oxazolidine **67** and oxidation.

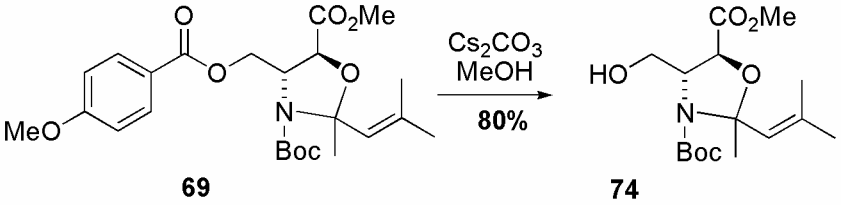

Figure 2.25 Trans-esterification of by-product **69**.

Oxidation of alcohol **73** to aldehyde **24** using Dess-Martin periodinane proceeded smoothly (Figure 2.24). Aromatic compounds were found to contaminate the product if the reaction was quenched for less than one hour using a reductive workup (an 8 : 2 (v/v) mixture of saturated aqueous sodium hydrogen carbonate and sodium thiosulfate solutions) and subsequent flash chromatographic purification led to decomposition and reduced yield. A much cleaner crude product was obtained by stirring the reaction for an hour after quenching and further purification was not necessary.

The NMR spectra of oxazolidine **67**, alcohol **73** and aldehyde **24** contained broad signals and some peaks were duplicated or shouldered. This was most evident in the spectra of aldehyde **24** where most signals were broad and many were missing, especially in the ^{13}C NMR. It was proposed that a dynamic equilibrium between two stable conformers was present and that they interconvert on the NMR time scale. NMR spectra were usually collected with the probe temperature set to 300 K. A ^{1}H NMR temperature study of aldehyde **24** was undertaken (Figure 2.27). Lowering the probe temperature to 280 K complicated the spectra further with two distinct sets of signals which can be clearly seen in an expansion of the spectra (Figure 2.28). Raising the probe temperature to 340 K merged these signals into one set. Lowering the probe temperature back to 300 K restored the spectra to its original condition. The ^{13}C NMR spectra changed in a similar way when exposed to the same temperature changes.

Similar observations were made by Garner and Park[44,45] when studying oxazolidine **75** (Figure 2.26). The authors proposed that the oxazolidine exists as rotamers which interconvert on the NMR time scale.

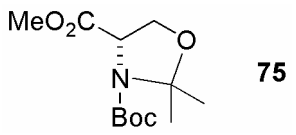

75

Figure 2.26 Garner and Park's oxazolidine.

This effect was observed for most derivatives of oxazolidine **67** and NMR spectra for characterisation were obtained at increased temperatures. With aldehyde **24** in hand, preparations for the modified Julia olefination were made.

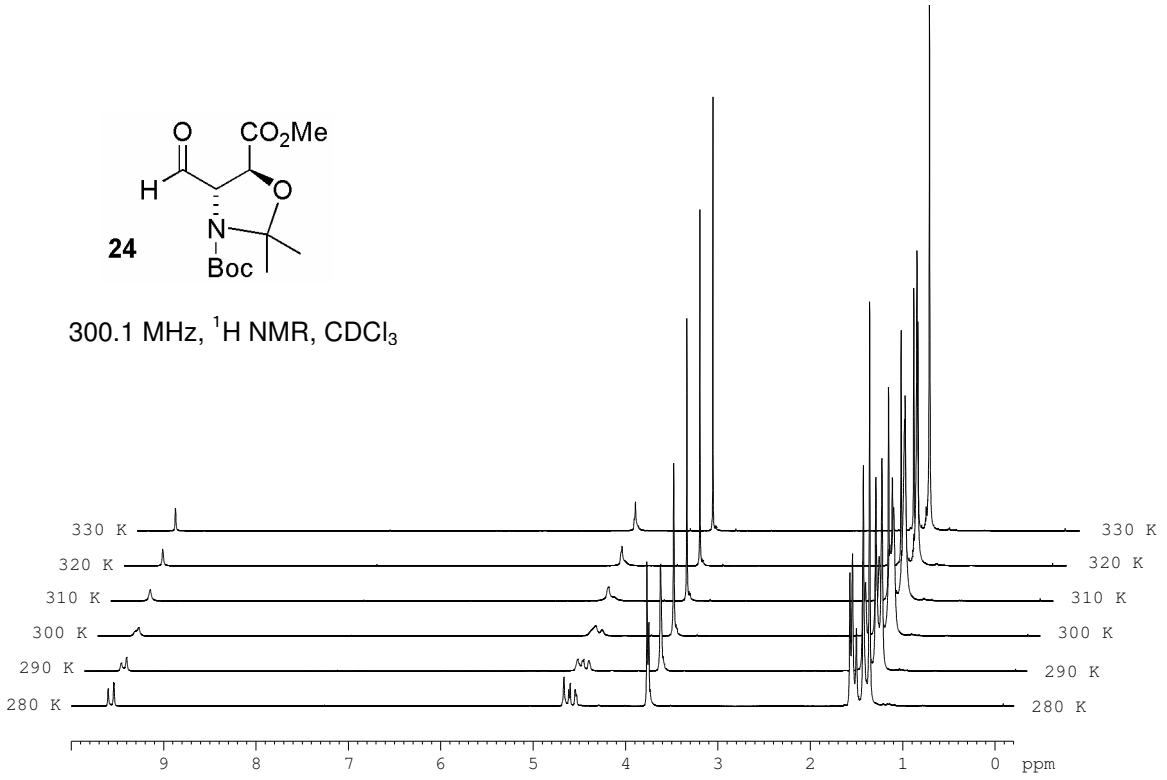

Figure 2.27 Variable temperature ^{1}H NMR of aldehyde **24**.

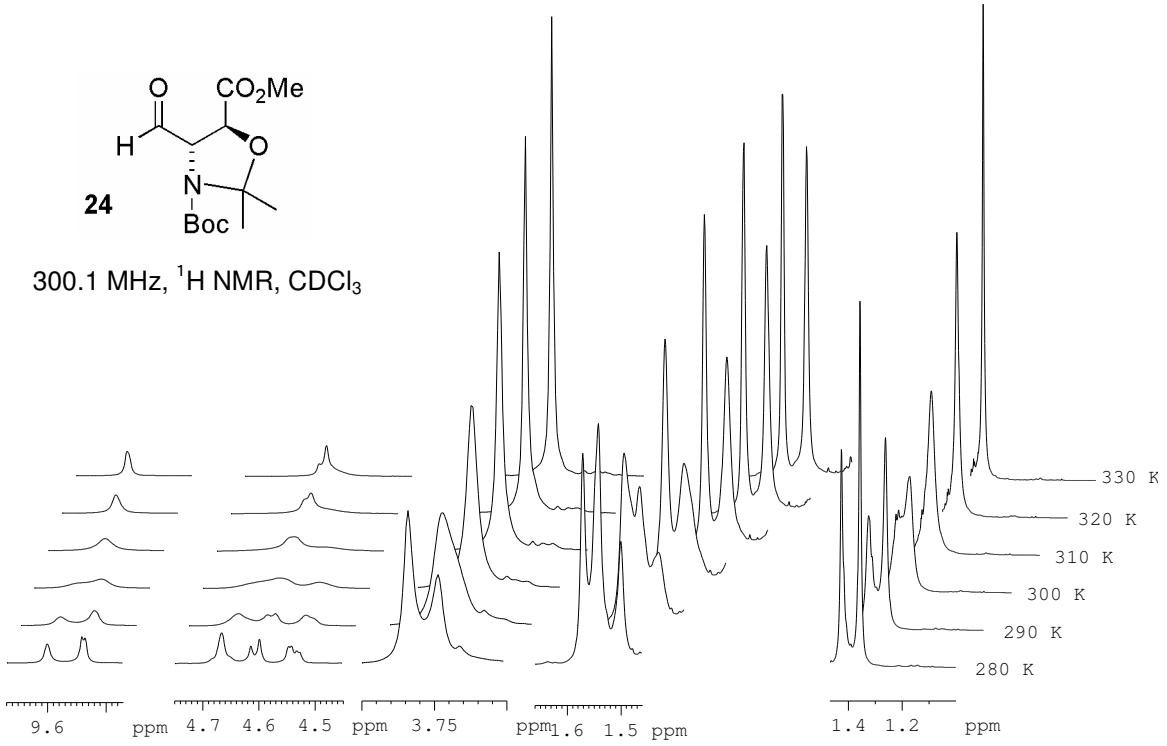

Figure 2.28 Variable temperature ^{1}H NMR of aldehyde **24** – expansion.

2.4 The Modified Julia Olefination

2.4.1 Introduction to the Reaction

In 1991, Sylvestre Julia and co-workers reported work into the reaction of metallated benzothiazol-2-ylsulfones with carbonyl compounds[46] which is now commonly known as the "one-pot" or "modified" Julia olefination (Figure 2.29). Organic chemists have recognised the potential of this chemistry as a powerful tool for the direct and economical synthesis of alkenes and have applied it frequently as a means of advanced fragment linkage in synthesis.[47] Many functional groups are tolerated in the reaction and choice of conditions can render the process highly selective for either the *trans*- or *cis*-alkene products. A very comprehensive review of the reaction was published by Blakemore in 2002.[47] Here the modified Julia olefination will be referred to as the "Julia olefination" and should not be confused with the "classical" Julia olefination.

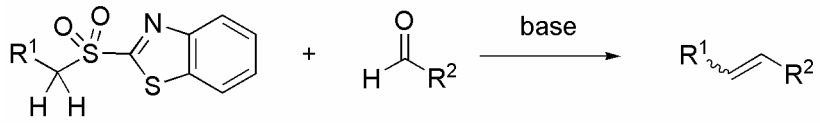

Figure 2.29 Generic modified Julia olefination.

The mechanism of the reaction (Figure 2.30) starts with reaction of heteroarylsulfone, shown here for the BT-sulfone, **76** with a strong, non-nucleophilic base, shown here for potassium bis(trimethylsilyl)amide (KHMDS), to form metallated heteroarylsulfone **77**. Addition of metallate **77** to aldehyde **43** occurs to form β-alkoxysulfone **78** which is inherently unstable because of the presence of the electrophilic imine-like moiety in the heterocycle. This compound is thought to undergo a Smiles rearrangement, which involves formation of spirocyclic intermediate **79** and subsequent opening of the spirocycle to form sulfinate salt **80**. Spontaneous elimination of sulphur dioxide and lithium benzothiazolone **81** affords the alkene products **51** directly.

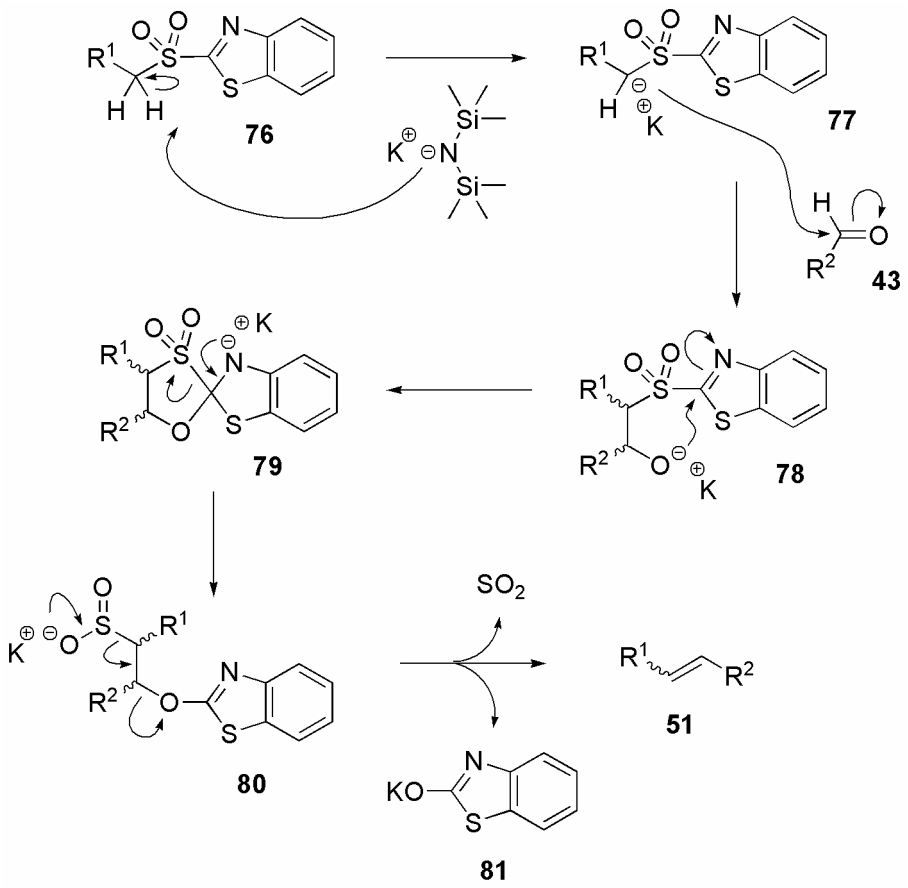

Figure 2.30 Mechanism of the Julia olefination.

The selectivity of the Julia olefination is often hard to predict with many factors influencing the stereochemical outcome of the reaction. Blakemore[47] has summarised the selectivity of the reaction for various types of substrates using BT-sulfones, although he claims that "the situation is certainly more complex" because there are experimental exceptions to his proposed rules. The following is a summary of Blakemore's observations (Figure 2.31).

Addition of simple sulfones to simple aldehydes, where R_1 and R_2 are alkyl groups, give simple β-alkoxy-BT-sulfone products ***anti*-78** and ***syn*-78** which have been shown to break down stereo-specifically to give olefin products *via* path **A**: the *anti*-isomer ***anti*-78** yields (*E*)-alkene ***E*-51** while the *syn*-isomer ***syn*-78** yields (*Z*)-alkene ***Z*-51**. The selectivity in this case is determined by the initial addition to the aldehyde and as a result often poor selectivity is obtained with these substrates.

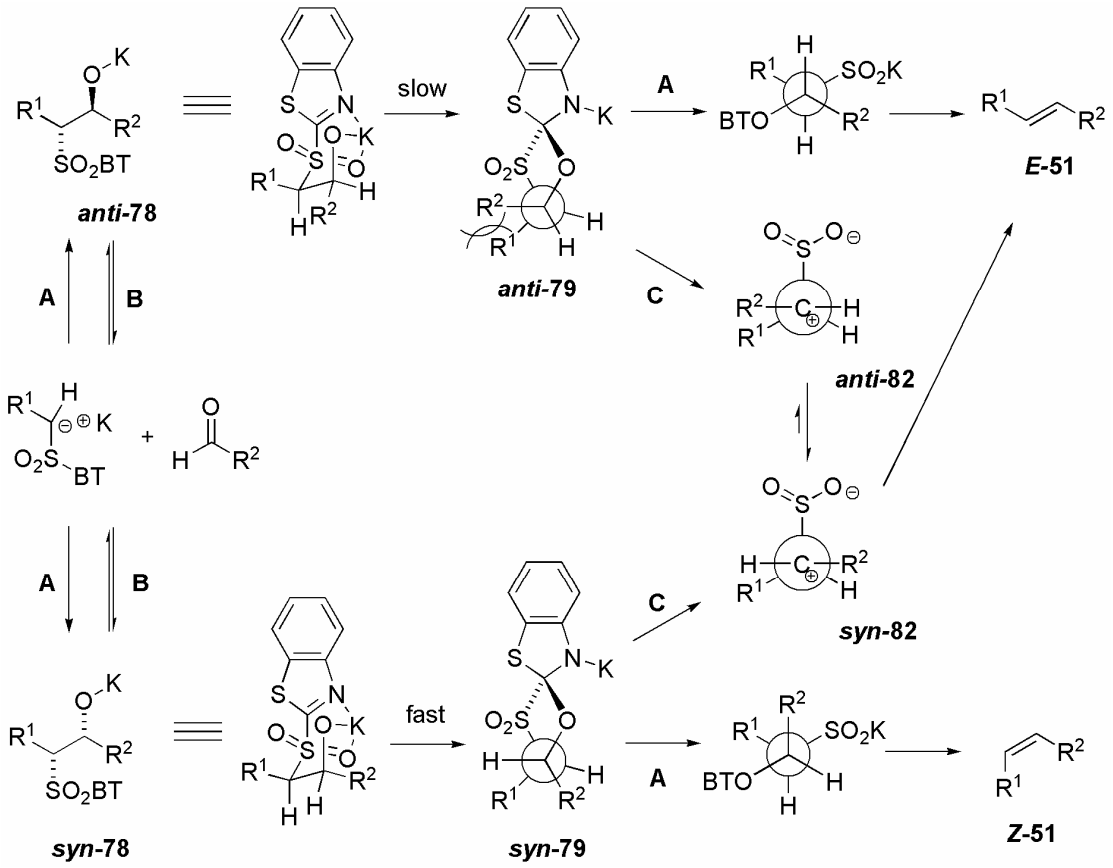

Figure 2.31 Selectivity in the Julia olefination.

β,γ-Unsaturated-BT-sulfones react with unbranched, aliphatic aldehydes to give alkenes with low to moderate (*Z*)-selectivity. In this case, addition to the aldehyde is a reversible process and the compound reacts *via* path **B**. The energy barrier to Smiles rearrangement for the *anti*-isomer ***anti*-78** is thought to be higher than that for the *syn*-isomer ***syn*-78** because of the eclipsed arrangement of R^1 and R^2 in the transition state for spiro-cyclisation. The equilibrium therefore favours cyclisation to ***syn*-79** and stereo-specific breakdown to give (*Z*)-alkene ***Z*-51**.

Electron rich aldehydes (α,β-unsaturated or aromatic) react to give alkenes with (*E*)-selectivity irrespective of what kind of BT-sulfone is used. Julia[48] proposed an alternative pathway where the spiro-cyclic compounds ***anti*-79** and ***syn*-79** breakdown *via* path **C**, to form betaine intermediates ***anti*-82** and ***syn*-82** respectively. The unsaturated residues in R_2 provide stabilisation for the carbenium ion present in these intermediates promoting this unusual pathway. Betaine ***anti*-82** equilibrates to favour the less sterically congested betaine ***syn*-82** which on loss of sulphur dioxide forms (*E*)-alkene ***E*-51**.

Use of different bases and solvents has been found to influence the selectivity of the reaction. The most commonly used system involves lithium diisopropylamide (LDA) as the base and tetrahydrofuran (THF) as the solvent at -78 °C. The choice of a non-nucleophilic base is essential to avoid ipso-substitution of the sulfone. The *trans*-selectivity of the reaction involving simple sulfones and aldehydes increases with solvent polarity and the electropositivity of the base counter-ion.[49] A combination of 1,2-dimethoxyethane (DME) as the solvent and potassium bis(trimethylsilyl)amide (KHMDS) as the base at -60 °C often provides optimal conditions. It was decided to use LDA and THF for the model reactions and the effect of varying the solvent and base was studied with the actual system.

Additives like hexamethylphosphoramide (HMPA) have been reported to modify the selectivity in the reaction.[50] Such experiments were not attempted because of the risks associated with handling this compound. Addition of HMPA or other additives like N,N'-dimethylpropylene urea (DMPU) or 18-crown-6-ether may increase the selectivity in the reaction.

The order of addition in the reaction has been found to influence the outcome of the reaction. Originally Julia olefinations were performed using "premetallation" conditions, as depicted in Figure 2.32, where sulfone **76** and the base, shown here for LDA, are reacted to form metallate **77** and aldehyde **43** is subsequently added to the reaction mixture. This protocol often works well, however if the sulfone readily self-condenses then low yields are obtained. An alternative protocol, known as "Barbier" conditions, involves addition of the base to a mixture of sulfone **76** and aldehyde **43** (Figure 2.33). This allows metallate **77**, which is formed *in situ*, to immediately add to the aldehyde reducing self-condensation. Complex aldehydes are often not compatible with such conditions and are often best reacted under premetallation conditions. Systems which involve complex aldehydes and sulfones which self-condense are best reacted using short premetallation times. It was decided to try both addition protocols in the model studies.

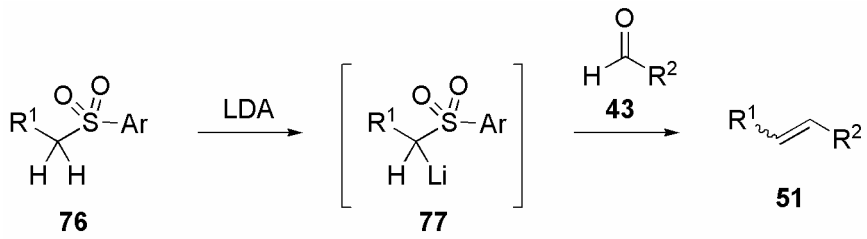

Figure 2.32 Premetallation conditions.

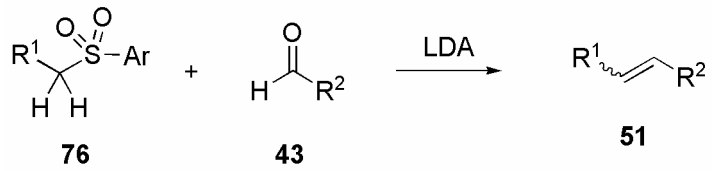

Figure 2.33 Barbier conditions.

BT-sulfones have been shown to be particularly susceptible to nucleophilic substitution at the *ipso*-position requiring the use of non-nucleophilic bases. This donor-acceptor nature of the sulfone enables the formation of self-condensation products.[47] This is especially a problem with sterically unencumbered sulfones like methyl BT-sulfone **83** that has been shown to readily self-condense to form compound **84** (Figure 2.34).[48]

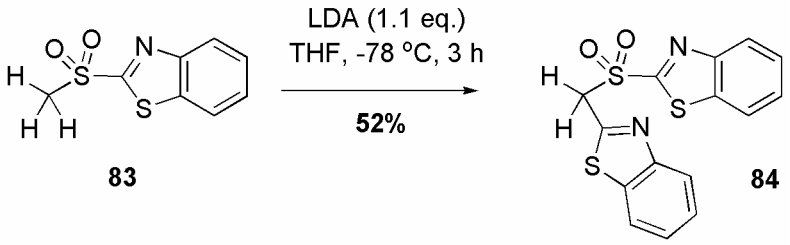

Figure 2.34 Self-condensation of methyl BT-sulfone.[48]

Since the initial use of BT-sulfones, many different heteroarylsulfones have been developed. The choice of heteroarylsulfone can influence the selectivity of the reaction with some favouring *trans*-alkene products while others favour *cis*-alkene products.[47] The two most commonly used *trans*-selective sulfones are the original benzothiazol-2-yl (BT) sulfone and the more recently developed 1-phenyl-1*H*-tetrazol-5-yl (PT) sulfone (Figure 2.35). The PT-sulfone was introduced by Kocienski and co-workers[49] and has been shown to be superior to the BT-sulfone in more than one way. It is generally more *trans*-selective when other

biasing electronic or steric factors are absent and it exhibits a reduced propensity to self-condense. It was decided to use both the BT- and the PT-sulfone in model studies to determine the reactivity and selectivity of each sulfone.

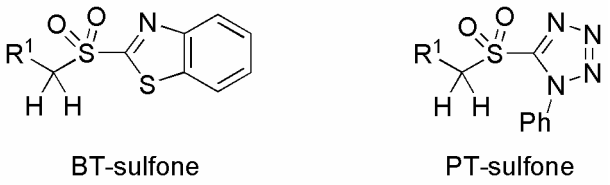

Figure 2.35 Generic BT-sulfone and PT-sulfone.

2.4.2 Preparation of Sulfones and Model Study

Hetero-aromatic sulfones, **25** and **26** were prepared from *p*-methoxyphenol in 3 steps using the same reaction sequence with an alternative source of hetero-aryl group (Figure 2.36).

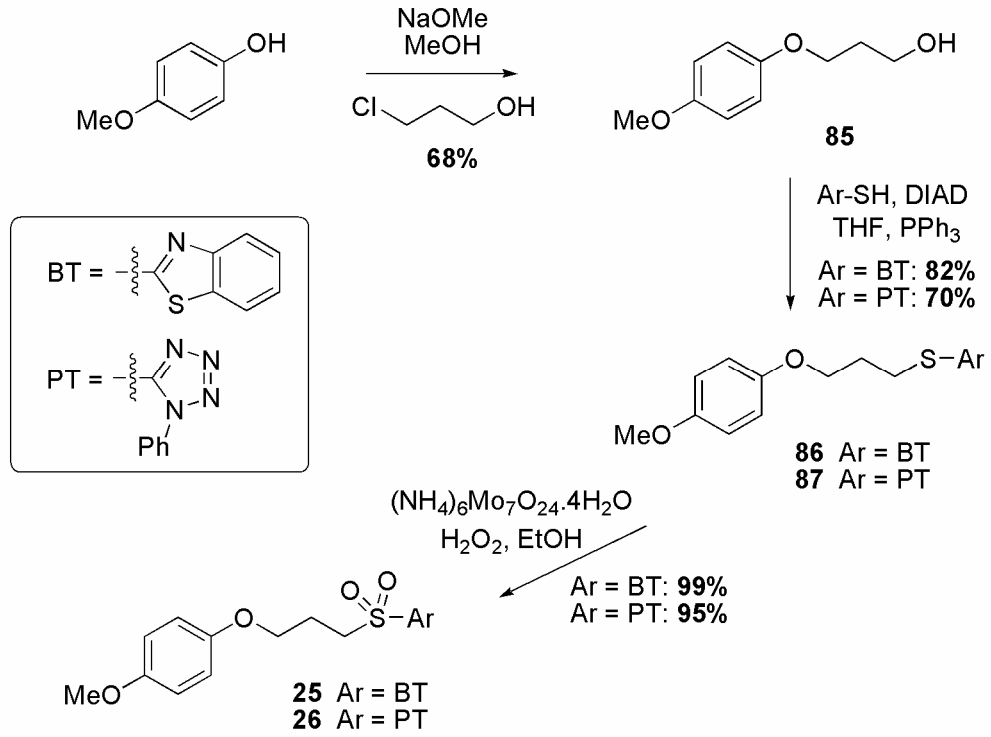

Figure 2.36 Preparation of sulfones.

Substitution of *p*-methoxyphenol on 3-chloropropanol gave ether **85**[69,70] in reasonable yield. Mitsunobu reaction between ether **85** and

2-mercaptobenzothiazole (BTSH) or 1-phenyl-1*H*-tetrazole-5-thiol (PTSH) gave thio-ethers **86** and **87** respectively. Oxidation of thio-ethers **86** and **87** using an excess of hydrogen peroxide with ammonium molybdate(VI) tetrahydrate as a catalyst gave sulfones **25** and **26** respectively. The oxidation reactions were monitored by TLC and the formation and subsequent disappearance of a more polar intermediate compound, assumed to be a sulfoxide, was observed.

A model study (Figure 2.37) using both BT-sulfone **25** and PT-sulfone **26** with isobutyraldehyde **88** to form alkene **89** was performed to compare the selectivity and reactivity of each sulfone in the Julia olefination. The importance of order of addition was studied by performing the reactions using both premetallation and Barbier conditions. PT-sulfone **26** was found to give superior *trans*-selectivity (Figure 2.38, entry 3, 4) over BT-sulfone **25** (entry 1, 2) under both addition protocols. An increased yield using Barbier conditions for both sulfones (entry 2, 4) indicated the benefits of this order of addition. Other products were observed in the reactions and were assumed to be self-condensation products. It was predicted from the model study that PT-sulfone **26** under Barbier conditions would give the best (*E*)-selectivity and yield for the reaction but it was decided to try both sulfones under Barbier conditions with the real system.

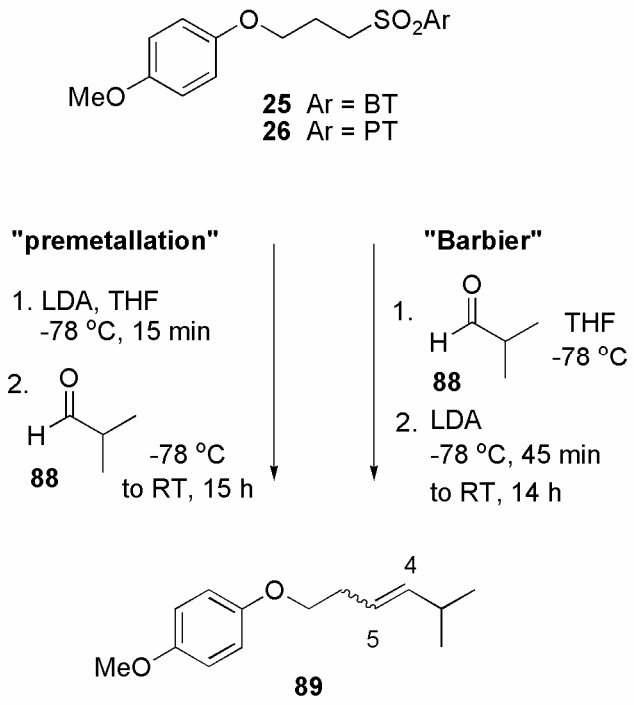

Figure 2.37 Model Julia olefinations.

Entry	Sulfone	Addition	Alkene **89**	
			Yield (%)	*E* : *Z**
1	**25**	premetallation	54	1 : 1
2	**25**	Barbier	71	1 : 1
3	**26**	premetallation	59	2 : 1
4	**26**	Barbier	67	2 : 1

* = determined by integration of the C_4-H and C_5-H peaks in the 200 MHz ^{1}H NMR spectra of the crude product

Figure 2.38 Results of model Julia olefinations.

2.4.3 The Reaction

A Julia olefination to form alkene **23** from aldehyde **24** (Figure 2.39) was performed using Barbier conditions in THF with LDA as the base. As predicted better (*E*)-selectivity was obtained with PT-sulfone **26** (Figure 2.40, entry 2) over BT-sulfone **25** (entry 1). The effect of solvent polarity and electropositivity of the base counter-ion on the selectivity of the reaction was briefly studied using the more polar solvent 1,2-dimethoxyethane (1,2-DME) in conjunction with sodium bis(trimethylsilyl)amide (NaHMDS, entry 3) or potassium bis(trimethylsilyl)amide (KHMDS, entry 4). The results were in agreement with previous studies[49] with the most (*E*)-selective conditions being 1,2-DME with KHMDS. The best yield was also obtained using these conditions. The low (*E*)-selectivity in these reactions is in agreement with Blakemore's summary of selectivity (for summary see Figure 2.31). Aldehyde **24** and sulfones **25** and **26** are all aliphatic and reaction would be predicted to occur *via* path **A** to form alkene **23** with poor (*E*)-selectivity.

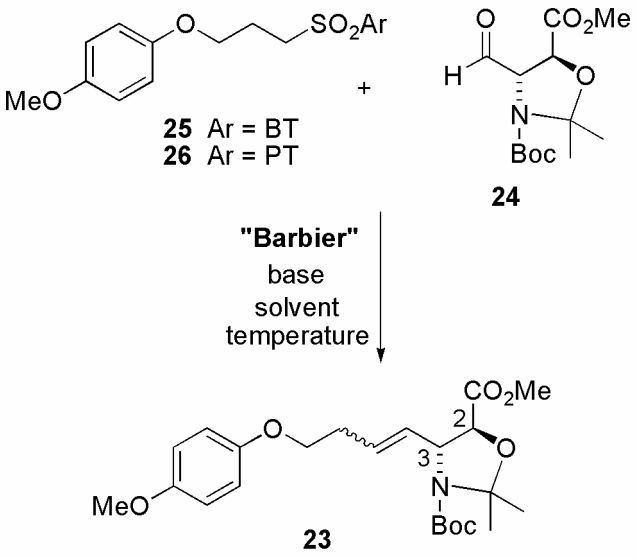

Figure 2.39 Julia olefination.

Entry	Sulfone	Solvent	Base	Temp. (°C)	Alkene **23**	
					Yield (%)	*E* : *Z**
1	**25**	THF	LDA	-78	42	1.2 : 1.0
2	**26**	THF	LDA	-78	35	1.6 : 1.0
3	**26**	1,2-DME	NaHMDS	-60	58	1.8 : 1.0
4	**26**	1,2-DME	KHMDS	-60	70	2.7 : 1.0

***** = determined by integration of the C_2-H and C_3-H peaks in the 200 MHz ^{1}H NMR spectra of the crude product. Where these signals were obscured by impurities, the ratio was determined from the ^{1}H NMR spectra of the isolated product

Figure 2.40 Results of Julia olefination.

(*E*)-alkene ***E*-23** and (*Z*)-alkene ***Z*-23** have very similar retention factors on silica with (*Z*)-alkene ***Z*-23** eluting first (Figure 2.41). Separation by flash chromatography was possible but often a large fraction contained mixtures of products and repeated chromatography was necessary. It has been reported that use of silver nitrate as a chromatographic absorbent can increase separation of alkene isomers.[51] An attempt to increase the separation of alkenes **23** using silver nitrate impregnated silica was made. TLC plates and silica were prepared and analysed by the methods of Li, Li and Li[52] (Figure 2.41). The order of retention was found to reverse on silver nitrate impregnated silica with (*E*)-alkene eluting

first. Flash chromatography using the silver nitrate silica did not give better separation with considerable streaking of the products. This modified separation was abandoned.

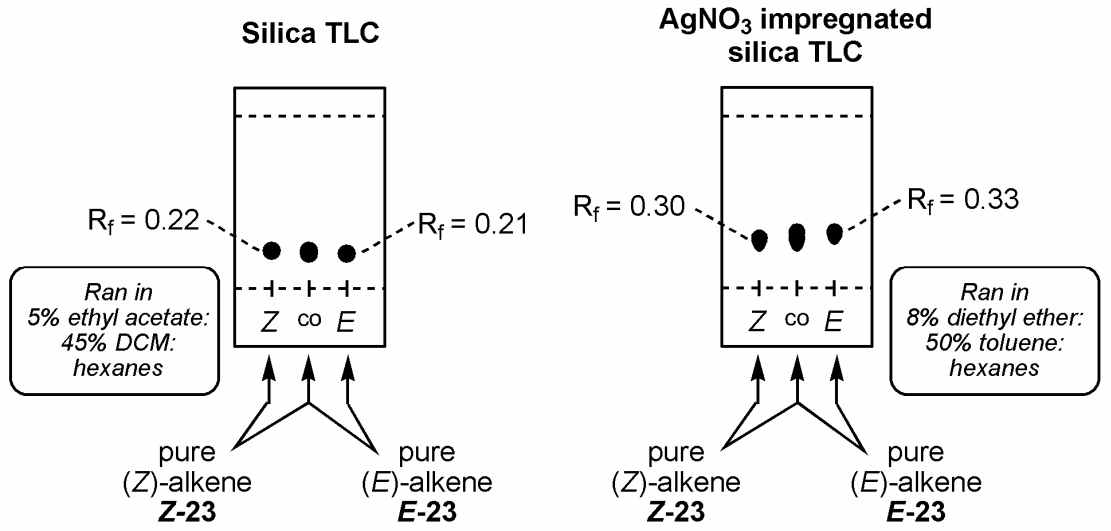

Figure 2.41 TLC-plates of alkene products.

The poor selectivity obtained in the reaction and the difficult separation lead to the decision that an alkene isomerisation reaction was necessary to improve the ratio of (*E*)-alkene ***E*-23** to (*Z*)-alkene ***Z*-23** in the mixture.

2.5 Alkene Isomerisation

Of the many alkene isomerisation procedures available[53] one involving treatment with thiophenol and azobisisobutyronitrile (AIBN) in benzene at reflux[54] was chosen. These conditions have been successfully used by Raghavan and Tony[55] to convert compounds with similar functionality. Reaction of the radical initiator AIBN with thiophenol forms thio-radical **90** (Figure 2.42) which adds reversibly across the double bond to form radical species **91A** and **91B** which readily interconvert between conformational isomers. Subsequent loss of thio-radical **90** regenerates the alkene. The success of the isomerisation relies on the greater thermodynamic stability of the less sterically congested (*E*)-alkene over the (*Z*)-alkene.

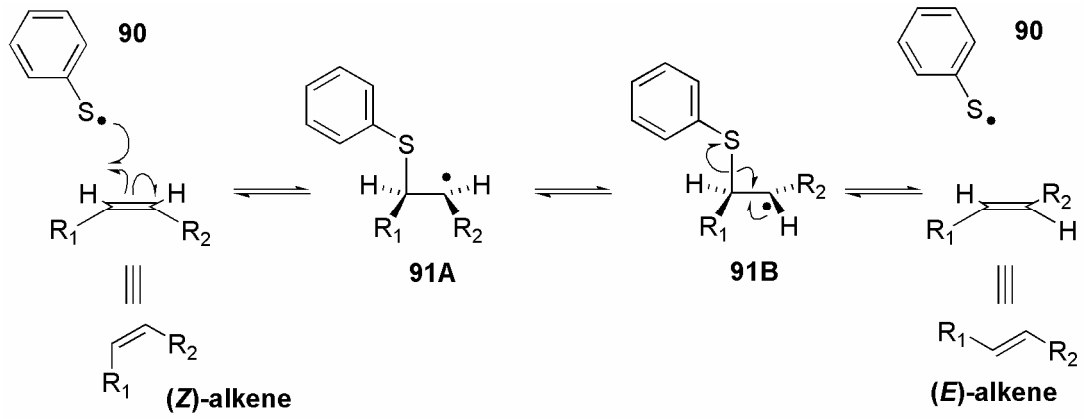

Figure 2.42 Mechanism of isomerisation.

A sample, enriched in (*Z*)-alkene ***Z*-23** after column chromatography, was isomerised (Figure 2.43) and the reaction was monitored by TLC. Good conversion was observed after 10 days at reflux when additional aliquots of AIBN were added to the reaction each day. (Note. AIBN has a half-life of 10 h in toluene at 65 °C)[56] The alkene mixture was recovered in essentially quantitative yield. When the reaction was analysed after shorter reaction times, intermediate ratios of isomers were observed. The enhanced ratio of (*E*)-alkene ***E*-23** in the product mixture made its separation by conventional flash chromatography more effective allowing isolation of pure (*E*)-alkene ***E*-23** as the major fraction.

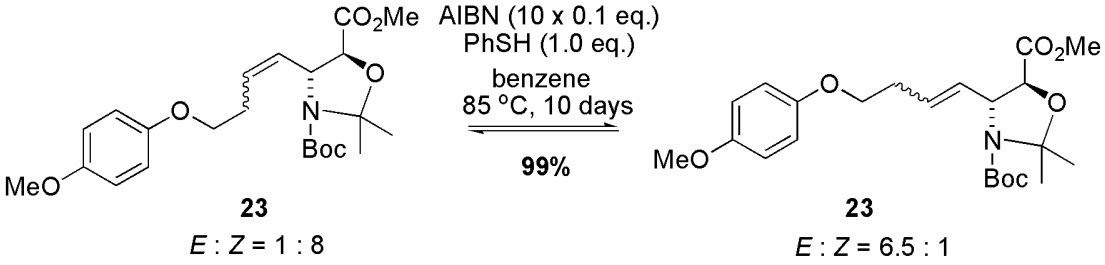

Figure 2.43 Alkene isomerisation.

In conclusion, (*E*)-alkene ***E*-23** was synthesised in nine linear steps, 27% overall yield and 97% ee. The focus of the project now turned to the next key step of the synthesis; the AD of (*E*)-alkene ***E*-23**.